Supplementary Materials

Hue Selectivity in Human Visual Cortex Revealed by Functional Magnetic Resonance Imaging

Ichiro Kuriki[1], Pei Sun[2], Kenichi Ueno[2], Keiji Tanaka[2] & Kang Cheng[2]

1. Research Institute of Electrical Communication, Tohoku University, Sendai, Japan.
2. RIKEN Brain Science Institute, Wako-shi, Japan.

Number of figures: 9

Number of movie: 1

Number of tables: 3

Supplementary text for the *Materials* section.

1. Psychophysical definition of chromatic detection thresholds.

Four squared checker-reversal patterns were shown in a two-by-two arrangement around the fixation point in the center of the screen. Each checker element sized 0.26° by 0.26° in visual angle and each square was 1.56° by 1.56° with a gap of 0.52° between the squares. Three of the four squares were reference stimuli, reversing at a temporal frequency of 5 frames per second (2.5 Hz) between the background gray and the gray with a 15% luminance increment. The target square reversed between the background gray and a test color that contained the increment in either L−M- or S-axis direction in addition to the 15 % luminance increment from the background gray. The location of the target square was randomized across trials. The measurements were made with the same apparatus used for the flicker photometry, and the isoluminance defined by the flicker photometry was used. The checker patterns were presented for 1 s. The subject was asked to report one of the four squares that appeared different from the remaining by pressing a button.

There were four staircase conditions: increment and decrement series for L-M and S-axis directions, respectively, which were presented in a randomly interleaved order. The contrast started from below the threshold in the incremental series and from above the threshold in the decremental series. The stimulus intensity was adaptively adjusted following the subject's response using a two-down and one-up procedure: it was decreased by a factor of 0.95 after two successive hit responses, and increased by a factor of 1/0.95 after a single failure of detection. The two staircases of incremental and decremental series eventually reached to an asymptote, and a threshold for each direction was defined by averaging the last five reversals of the staircase before reaching the asymptote.

2. Formulae for the definition of stimulus chromaticity.

Below we provide the detailed formulae for the derivation of color stimulus. The formulation of color-stimulus *c* in cone-response representation under an isoluminant constraint is as follows:

$$\begin{aligned} L_c\left[\phi(t)\right] &= \left\{1 + L_{amp}\cos\left[\phi(t)\right]\right\} L_b \\ M_c\left[\phi(t), \omega_{sub}\right] &= L_b + \omega_{Sub} M_b - L_c\left[\phi(t)\right] \\ S_c\left[\phi(t)\right] &= \left\{1 + S_{amp}\sin\left[\phi(t)\right]\right\} S_b \end{aligned}, \quad \text{(S1)}$$

where $\phi(t)$ represents the phase of a stimulus cycle as a function of time. L_{amp} and S_{amp} represent the radii of the oval trajectory along $\Delta L/L_b$ and $\Delta S/S_b$ axes, respectively. Subscript *c* for the L_c, M_c, and S_c represent cone responses of chromatic components for L, M, and S-cone, respectively. A factor ω_{sub} for M-cone response represents the *relative M-cone weight* for each subject, as mentioned above: $L + \omega_{sub} M$ represents the luminance channel output in the subject. Thus, the chromaticity of the hue-changing locus in ($\Delta L/L_b$, $\Delta S/S_b$) coordinates is given as follows:

$$\begin{aligned} \Delta L/L_b &= \left(L_c\left[\phi(t)\right] - L_b\right)/L_b \\ \Delta S/S_b &= \left(S_c\left[\phi(t)\right] - S_b\right)/S_b \end{aligned}. \quad \text{(S2)}$$

M-cone response is not mentioned, which was uniquely defined under the constraint of isoluminance. These cone excitations before the application of luminance pedestal (Formula S2) were used to calculate the chromaticity in the cone contrast space (Figure 1A). S-cones are considered irrelevant to the luminance channel (Eisner and MacLeod, 1980). However, changes in L- and M-cone responses only would result in the shift in color along the S-axis in Figure 1A. Thus, we manipulated all three cone-responses by the same factor, meaning that the stimulus' chromaticity was invariant after luminance pedestal was applied. Accordingly, the cone responses after the application of 15% luminance pedestal become:

$$\begin{aligned} L_{cS}\left[\phi(t)\right] &= L_c\left[\phi(t)\right] \times 1.15 \\ M_{cS}\left[\phi(t), \omega_{sub}\right] &= M_c\left[\phi(t), \omega_{sub}\right] \times 1.15 \\ S_{cS}\left[\phi(t)\right] &= S_c\left[\phi(t)\right] \times 1.15 \end{aligned}. \quad \text{(S3)}$$

The subscript *cS* on the left side of each equation stands for a cone response to the color stimulus generated with 15% luminance increase. The obtained cone responses [L_{cS}; M_{cS}; S_{cS}] were first transformed to CIE XYZ (1931) by applying the Smith-Pokorny's cone fundamentals (Smith and Pokorny, 1975).

Supplementary Figures

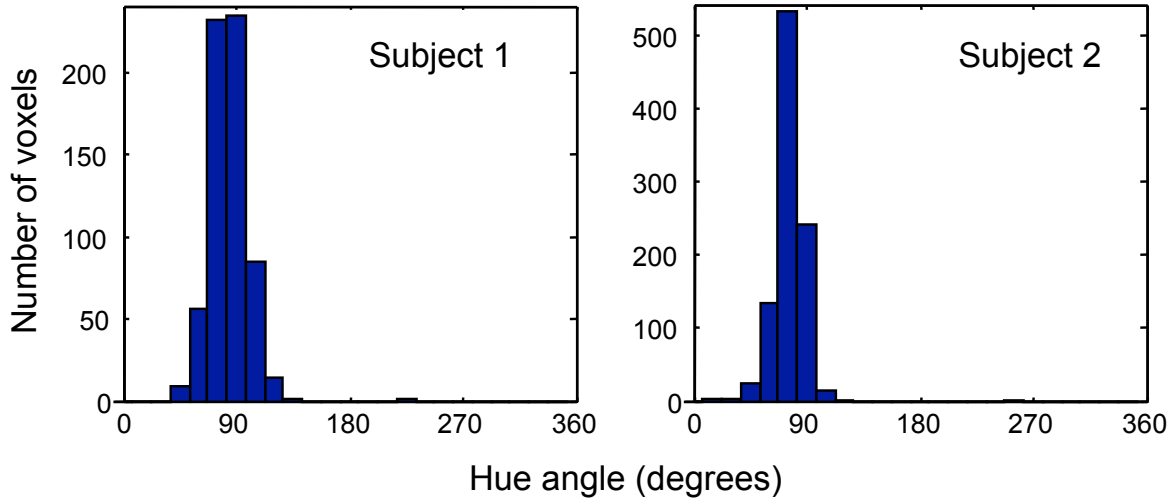

Figure S1. Histograms of activated voxels obtained in a control luminance-modulation experiment.

Instead of color changes over time around the hue angle (360°), we modulated the luminance of the stimulus, whose configuration was otherwise identical to the stimulus used in the main experiment (reversal between luminance-modulated checker elements and gray background at a temporal rate of 5 frames per second). Atop of the 15% luminance pedestal, additional luminance between 0 and 8% was added to the checker elements, which was sinusoidally modulated with a cycle of 24 s. The peak luminance (15+8%=23%) appeared 6 s (=1/4 cycle) after the onset of the stimulus, which was expected to evoke a maximum BOLD response. The criteria for selecting activated voxels in this experiment were the same as those for analyzing chromatic modulations in the main experiment (see Experimental Procedures, Data Analysis section in the main text): the threshold for the r^2 value was 0.15, the SNR for the luminance modulation at the frequency of 1/24 Hz was 8.3 dB, and the amplitude of BOLD signal for each of the two hemodynamic responses before the differential hemodynamic responses was obtained was set to be less than 5%. The results from both subjects exhibit a sharp peak response around 90° in the hue angle (at 1/4 cycle). The hemodynamic delays in both histograms were individually corrected based on the time when the expected peak response appeared; the same corrections were also made for respective subjects in the main chromatic modulation experiment.

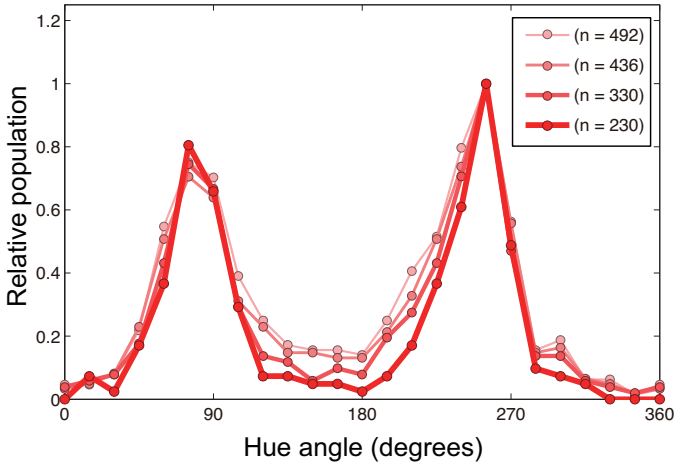

Figure S2. The shape of hue-selective histogram does not depend on the number of voxels. Using the example shown in Figure 2A, we systematically lowered the SNR (signal to noise ratio) threshold from 8.3 [dB] (Figure 2A, *right*), to 5.0, 1.0 (Figure 2A, *left*), and 0.0 [dB], resulting in voxel numbers of 230, 330, 436 and 492, respectively. Their corresponding histograms are shown above, where the line width increases with the increasing SNR threshold, with 8.3 [dB] being the thickest. The four histograms, normalized to their respective maxima, were not significantly different (Kolmogorov-Smirnov tests between histograms generated with SNR threshold of 0, 1, and 5 [dB], respectively, and that generated with SNR threshold of 8.3 [dB], all $p > 0.89$).

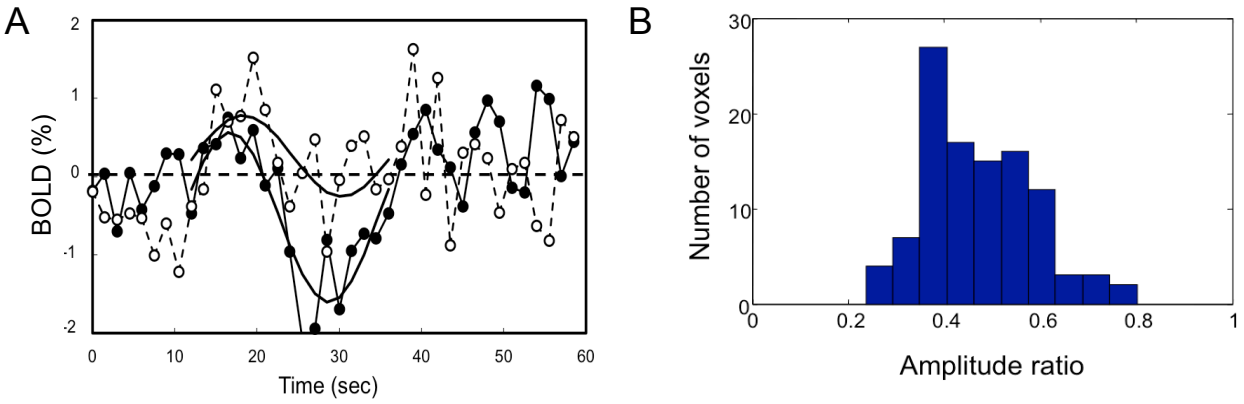

Figure S3. Differential hemodynamic response observed in the present study reflects primarily the modulation of chromatic component in the stimulus.

In order to examine whether the BOLD modulation observed in the main experiment was indeed related to the color modulation, we conducted a control experiment with the chromatic modulation along the same hue-circle but half the radius with respect to the radius used in the main experiment. We reasoned that if the chromatic component of the stimulus evokes the BOLD response, the amplitude of the BOLD response should be reduced by approximately 50% when the radius is halved, if the assumption of partial linearity holds (Boynton et al., 1996). In a single functional scan, we used two series of stimuli as in the main experiment (namely, one series starting 0° in the hue angle, and the other starting from 180° in the hue angle), each of which was presented either in the radius identical to that used in the main experiment (i.e., $\Delta L/L_b = 0.08$ and $\Delta S/S_b = 0.80$) or in half of that radius (i.e., $\Delta L/L_b = 0.04$ and $\Delta S/S_b = 0.40$). (A) shows typical differential hemodynamic responses to the full-radius stimuli (filled circles) and half-radius stimuli (open circles), respectively, from a representative voxel. The amplitude of sinusoidal modulation was estimated by fitting a cosine curve to each hemodynamic response (solid curve for full-radius stimuli; dashed curve for half-radius stimuli). We compared the two amplitudes by taking the ratio between the two; for the example voxel shown in (A), the ratio is 0.554. For population analysis, the selection criteria for activated voxels were the same as those used in the main experiment (see Experimental Procedures, Data Analysis section in the main text): the threshold for the r^2 value was 0.15, the SNR for the luminance modulation at the frequency of 1/24 Hz was 8.3 dB, and the amplitude of BOLD signal for each of the two hemodynamic responses before the differential hemodynamic responses was obtained was set to be less than 5%. In addition, only the voxels with the difference in hue-selectivity between the two radius conditions smaller than 15° were further analyzed. (B) shows the distribution of resultant ratios across 106 selected voxels from Subject 1's V1. Although the standard deviation (S.D.) of the distribution is not negligible, the mean is 47.7% (mean ± S.D.; 47.7 ± 11.45%), close to what can be expected from a partial linearity. The result from this control experiment thus supports our conclusion that the differential BOLD response observed in the present study reflects primarily the modulation of chromatic component in the stimulus.

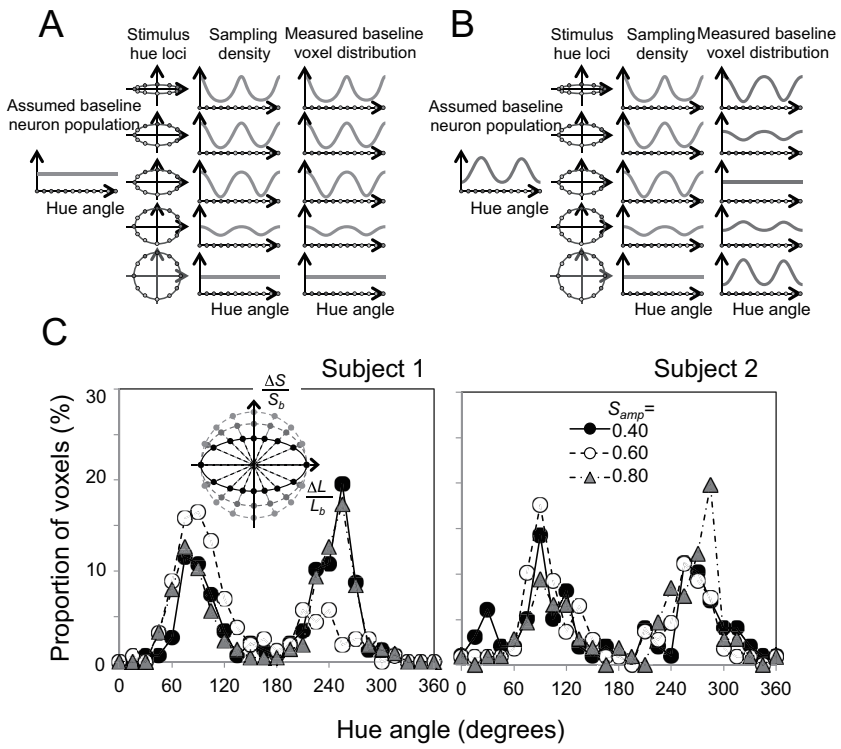

Figure S4. Effects of hue-sampling density on hue-selective histograms.
Panels (A) and (B) schematically illustrate expected hue-selective histograms as a consequence of the neuron-population bias in color selectivity and the sampling-density difference between various S_{amp} conditions. Assuming neurons selective for different hues are equally distributed (A), if the sampling density in the hue angle matches the population density of hue-selective neurons when L−M and S-axis stimulations are equated by the multiples of discrimination threshold (i.e., L_{amp} = 0.08 and S_{amp} = 0.80), this over-representation is not expected. If it were the case, we should have observed an over-representation around L−M cone selective directions (0°/180°), rather than 90°/270°, in most conditions (Figures 2C-2E). Instead, if the variability among hue-selective neurons is uneven and abundant around the S axis, as illustrated in panel (B), then this population difference will be reflected in the histogram when all neurons are equally sampled in the hue angle defined on a circle of radii with L_{amp} = 0.08 and S_{amp} = 0.80, meaning that the intrinsic population difference can constitute a bias around the S axis. In each panel, the leftmost column shows the color selectivity of a hypothetical neuron population to be sampled (A, equally distributed; B, bias around 90° and 270° in the hue angle), the middle two columns show the systematic change in the sampling density following the change in the value of Samp, and the rightmost column shows resultant histograms under various S_{amp} conditions. (C) shows histograms measured in V1 for Subjects 1 and 2 under three conditions of S_{amp} (0.40, 0.60, and 0.80) while keeping the sampling hue angles unchanged (equally sampled along the circumference of Lamp = 0.08 and Samp = 0.80). Each histogram was normalized by the total number of voxels that passed selection criteria. Statistically significant differences were tested for each subject's normalized histograms between S_{amp} conditions by two-sample Kolmogolov-Smirnov test. Although a significant difference was observed in Subject 1 between S_{amp} = 0.40 and others ($p < 0.05$), it is clear that the three conditions are essentially similar: even the result under S_{amp} = 0.40 for Subject 1 exhibits prominent peaks around 90 and 270 degrees, indicative of the over-representation around S-cone axis.

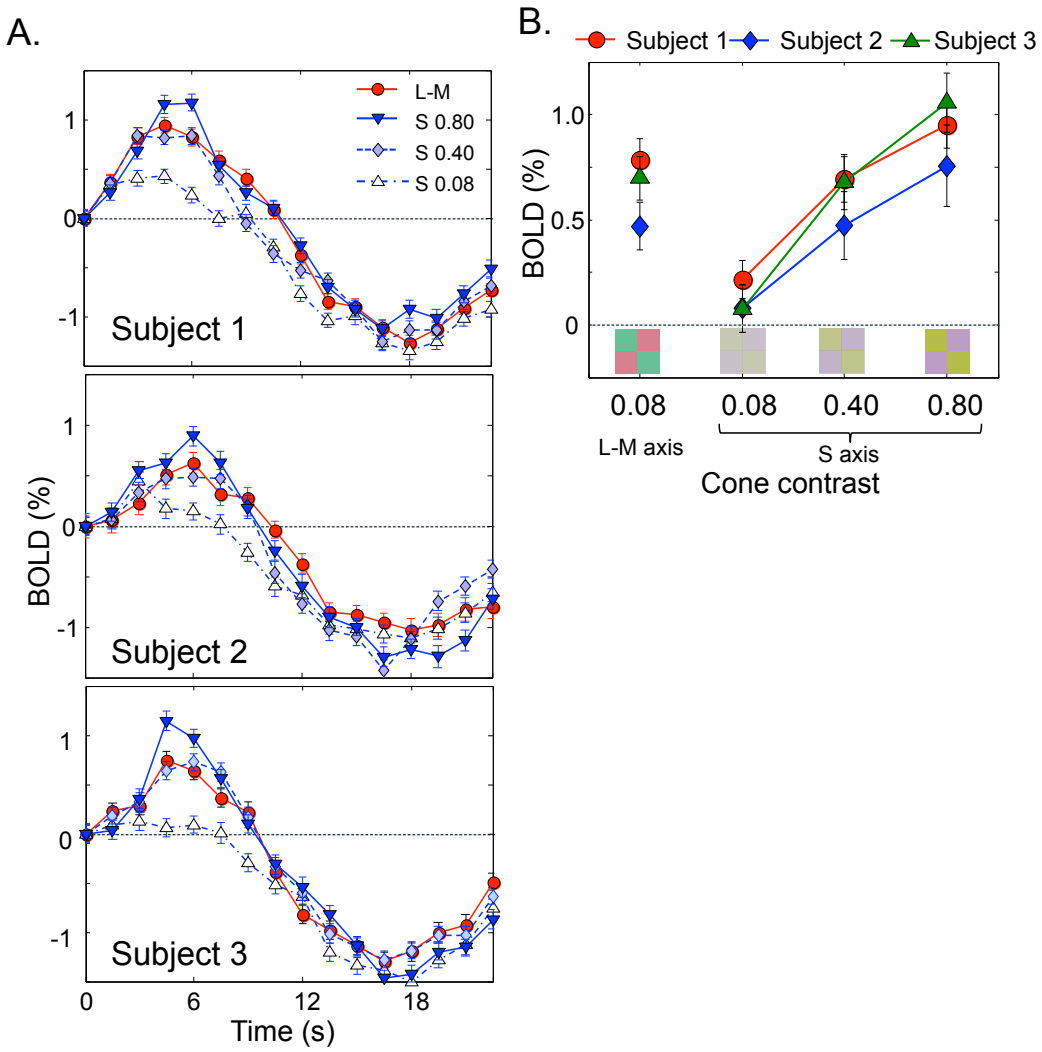

Figure S5. Minimizing possible population bias among hue-selective neurons.
Based on Figure S4, it may be possible to consider dissecting the trend in the histograms into two components: a base trend with peaks around either 0°/180° or 90°/270°, and the remainders. In order to uncover the presence of true peaks and troughs in the histograms, it is necessary to remove this base bias around the S-cone axis. Indeed, it has been reported that, when L_{amp} and S_{amp} are equated with the multiples of detection thresholds, hues around the S axis evoke larger BOLD responses than hues around the L−M axis do (Engel et al., 1997a; Mullen et al., 2007). We thus sought to find a condition, in which the strengths of evoked BOLD responses to L_{amp} (kept constant at 0.08) and S_{amp} (0.04, 0.40, or 0.80) would be equated, by performing the following experiment. For each S_{amp} condition, on a single-voxel basis, we derived amplitudes of BOLD responses to isoluminant stimulus, similar in size and temporal property to those in the main experiment, presented for 1.5 s along L−M axis and S axis. Figure S5A shows obtained hemodynamic responses averaged across V1 voxels that met selection criteria for all S_{amp} conditions in three subjects (59, 50, and 39 voxels, respectively).

Figure S5B shows averaged BOLD responses around the peak (t = 6-7.5 s) for all three conditions in V1 for each subject. A one-factor analysis of variance (ANOVA) with multiple measures revealed that the main effect of S_{amp} conditions was statistically significant (all $p < 0.05$): $F(2,174) = 8.93$ in Subject 1,

$F(2,147) = 3.28$ in Subject 2, and $F(2,114) = 4.80$ in Subject 3. According to the multiple comparisons with t-test for the post-hoc analysis between Samp conditions, significant differences were observed between $S_{amp} = 0.08$ and 0.80 conditions ($p < 0.05$) in all subjects. The S_{amp} value that would evoke an equal BOLD response with the L-M stimulus with $L_{amp} = 0.08$ was obtained by the linear interpolation between the data points in each subject. The equilibrium S_{amp} values for Subjects 1-3 were 0.543, 0.396 and 0.419, respectively. The result from this analysis suggests that the bias to either of the two axes, on average, was the minimum at S_{amp} of 0.453, thus resulting in a L_{amp} (0.08) : S_{amp} (0.453) ratio of 1 : 5.66.

This ratio is slightly larger than those reported in the previous studies. Assuming a partial linearity exists between the strength of stimulation and the amplitude of evoked BOLD response (Boynton et al, 1996), it is possible to estimate the amplitude of BOLD response by an S-cone stimulation that matches the amplitude of L-cone stimulation. The estimation for the results reported in Mullen and colleagues (2007, measured from their Figures 5 and 6) led to an aspect ratio of L−M : S = 1 : 2.75, while the aspect ratio of iso-fMRI signal contour (L−M : S) in Engel and colleagues (1997a, measured from their Figures 2 and 3) ranged from 1 : 2.18 to 1 : 4.87. This ratio does not exactly match the condition in our study that resulted in the smallest BOLD amplitude bias between the L−M and S-cone axes in the hue-selective histogram ($L_{amp} = 0.08$ and $S_{amp} = 0.453$, or L−M : S = 1 : 5.66, on average). However, they all agree that the S-cone stimulation matched with either cone contrast or multiples of thresholds do not evoke equal responses in terms of the BOLD amplitude.

Taking a number of differences between different studies into consideration, such as the difference in the spatiotemporal profile of stimuli, the 15% luminance pedestal used in our study, as well as the difference in the subjects, the similarity in the trend of the ratios estimated from different studies suggests that an over-representation of hue-selective neurons around the S-cone-selective axis may indeed exist. The higher population density around the S-cone axis in the histogram implies the presence of large variability in the preferred hue among neurons. Consequently, the histogram acquired with this sampling density is considered to depict a relatively unbiased population trend across the hues and contains additional peaks away from cone-opponent axes.

Our finding that a possible over-representation of hue-selective neurons around the S-cone axis exists when L−M and S axes are equated with the color-detection thresholds was rather unexpected. To our knowledge, this has never been documented previously in either monkey studies or human studies. The large modulation in the histogram with two cycles per hue-circle, however, may be related to the previously observed asymmetry in the amplitude of BOLD responses to the hues around the L−M axis and those around the S axis (Engel et al., 1997a; Mullen et al., 2007). In our study, the quantification for the histograms was on the number of hue-selective voxels, which were determined based on certain selection criteria but without considering the amplitude of the BOLD signal. However, the population of neurons that respond to stimuli along a hue-selective axis should affect the average BOLD signal intensity within a ROI, which can be estimated by the total BOLD signal intensity divided by the number of voxels in the ROI. Therefore, for a ROI (e.g., a visual area) with a given total number of voxels and multiple neuron populations, the larger the number of voxels in a population is, the larger the total BOLD amplitude the population evokes. Color changes along the L−M or the S-cone selective axis may stimulate all kinds of neurons fed by the L−M or S-cone inputs, respectively, regardless of the exact hue selectivity of each neuron.

Future studies on both humans and non-human primates are warranted in elucidating the nature of over-represented neuron populations, their functions in color-coding, as well as their roles in color perception.

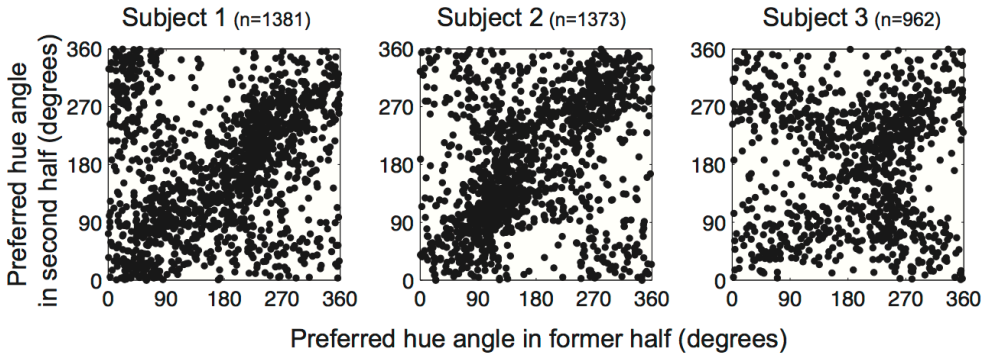

Figure S6. Voxel-by-voxel reproducibility of preferred hues.
To examine the voxel-by-voxel reproducibility of the hue selectivity within a run, we split images in a run into the former and latter halves, each containing images acquired during 5 repetitions of stimulus block A and block B. If the hue selectivity was consistent within a run, similar hue selectivity should be observed from the two halved datasets. For each half of the run, we used the same approach to identify the voxels that were selective for different hues, and then estimated the reproducibility between the results obtained in the two halves. Although overall the numbers of hue-selective voxels in both halves decreased due to the reduced SNR (data points were halved), reasonable and significant voxel-by-voxel reproducibility was found in all three subjects (voxels from all four visual areas in all four runs used in Figures 3 and 4 were pooled, resulting in 1381, 1373, and 962 total voxels from the three subjects, and circular correlation coefficients (Berens, 2009) were $\rho=0.388$ for Subject 1, $\rho=0.411$ for Subject 2, and $\rho=0.227$ for Subject 3; all $p<0.001$ for the test of correlation coefficient against zero correlation). In the three panels for Subject 1, Subject 2, and Subject 3, respectively, horizontal and vertical axes represent the preferred hue angle estimated in the first and second half, respectively. Note that hues around 0° and those around 360° in these plots are continuous in the hue circle.

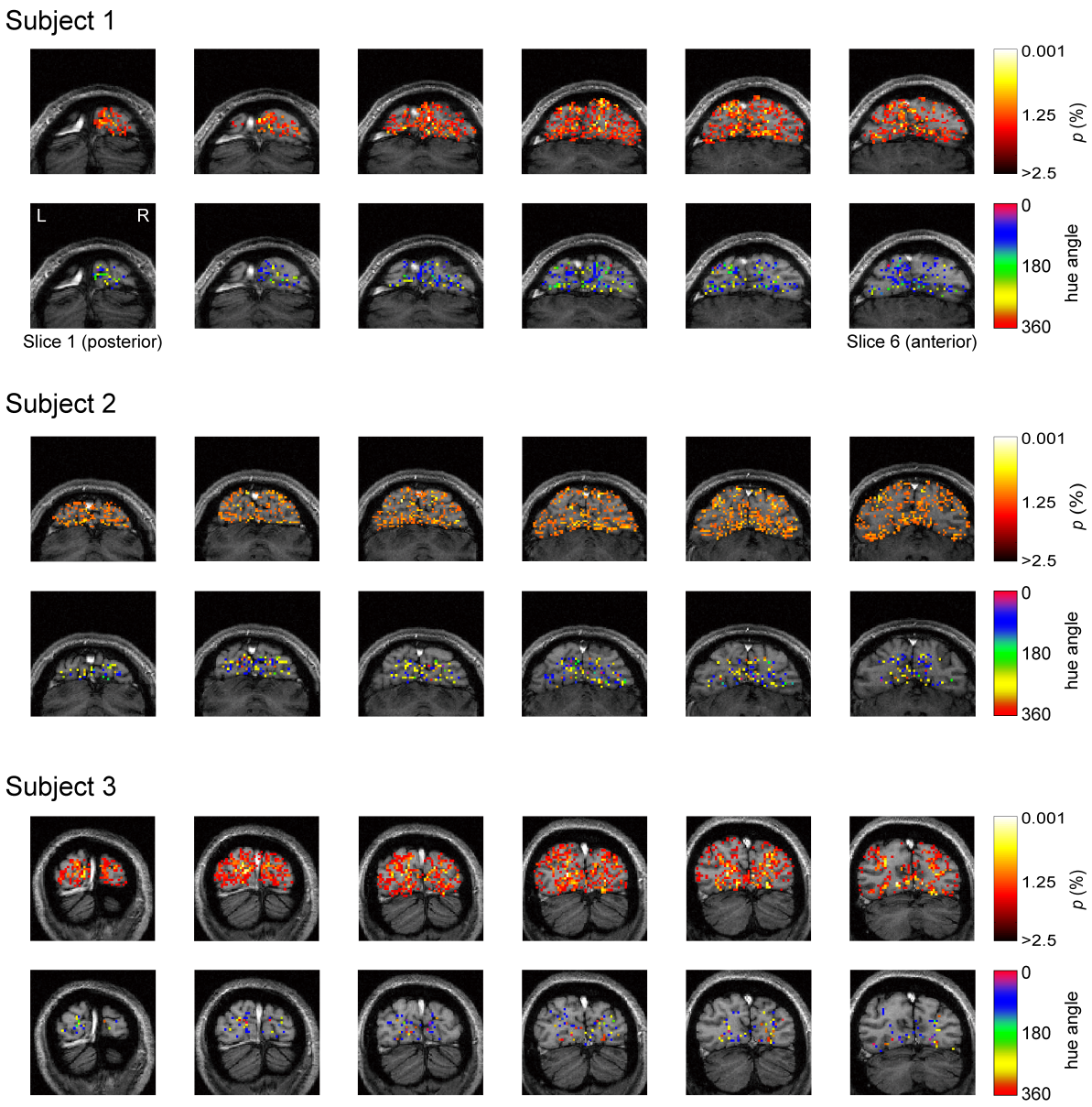

Figure S7. Comparisons of visually responsive and hue selective voxels.
For each subject, visually responsive voxels in a representative run are shown in the upper row and hue-selective voxels are in the lower row (see Methods section, "Data Analysis" subsection in the main text for procedures selecting these voxels). The left- and right-most panels correspond to the most posterior and anterior slices, respectively. For technical reason, we did not create a surface-rendered flat map for hue-selective voxels, because when a surface map is created, there is an inevitable processing step of summarizing information from the voxels that differ in the cortical "depth." Averaging is typically involved; however, we consider it inappropriate to average the phasic information in our case, i.e., preferred hues. Areal dividends (V1 through V4) of hue-selective voxels, as proportions of visually responsive voxels in respective areas, are summarized in Table S3.

By comparing visually responsive voxels with hue-selective voxels, it is clear that only a small fraction of visually responsive voxels were hue-selective (see the **row in bold letters** for the fraction of

hue-selective voxels in Table S3). It is also clear that hue-selective voxels are sparsely and separately distributed and there is no obvious clustering of hue-selective voxels at this spatial scale. These observations are consistent with our reasoning that hue selectivity may be revealed by biased sampling of color domains in the human visual cortex using fMRI (see Introduction section in the main text).

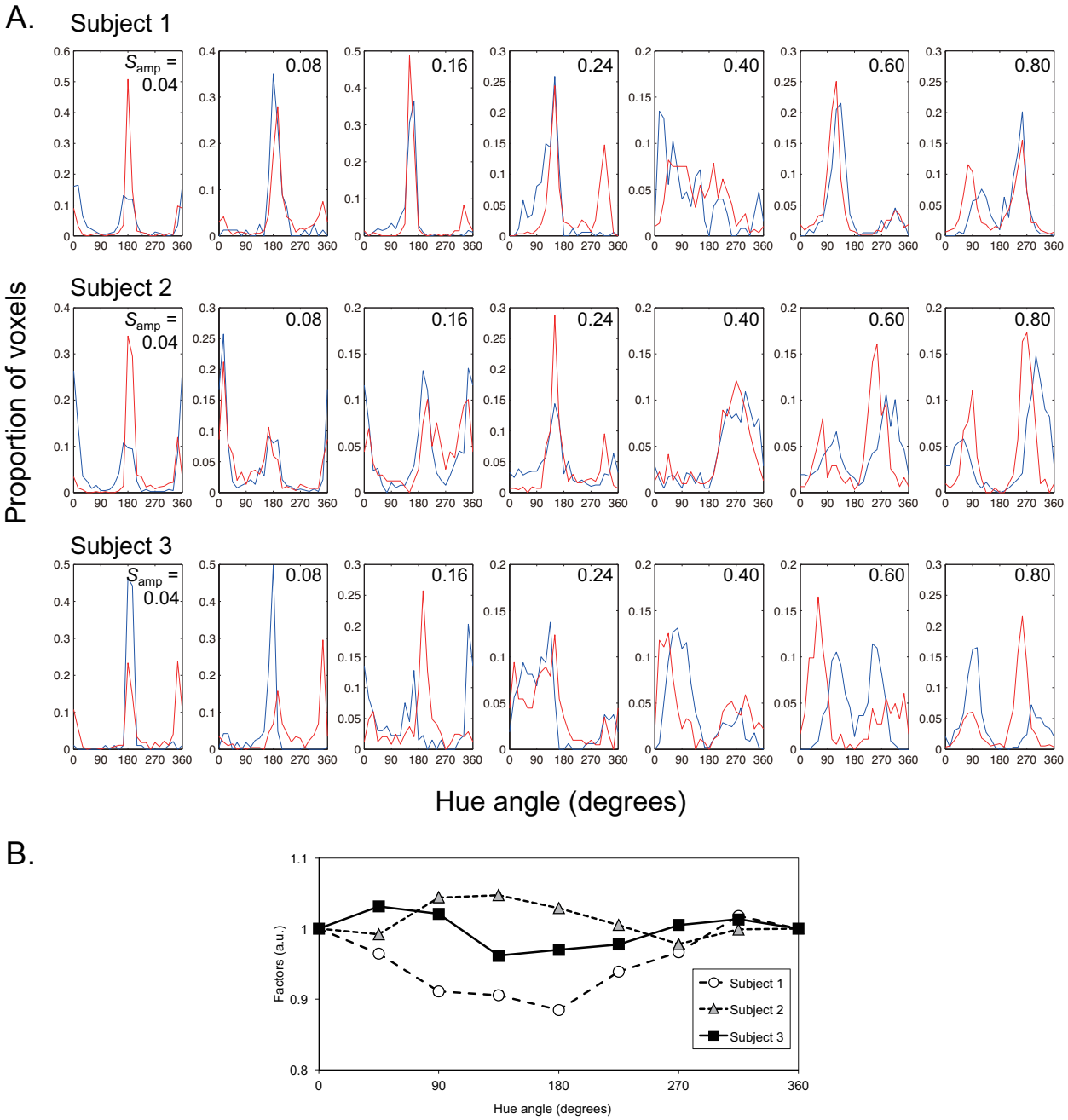

Figure S8. Hue-selective histograms obtained under isoluminance defined by minimum flicker at 2.5 and 16 or 20 Hz.

Because the test stimulus was alternating between the background gray and color at 2.5 Hz, with a 15% luminance pedestal, the mechanism sensitive to color could evoke the difference in strength of response among hues equated for luminance (isoluminance), defined by minimum flicker at 16 or 20 Hz, depending on subject. To address this issue, the results from a series of measurements, similar to those shown in Figures 2C-2E, were obtained with hue changes under minimum flicker at 2.5 Hz. In panel (A), blue traces are the results from 16 or 20 Hz and red traces the results from 2.5 Hz. The similarity of the two histograms was evaluated by Pearson's correlation coefficients averaged across seven S_{amp} conditions

in each subject: 0.667 for Subject 1, 0.594 for Subject 2, and 0.316 for Subject 3. Although the coefficient in Subject 3 is slightly lower than those in other two subjects, typical hue-selective characteristics, such as the selectivity for intermediate hues, are prominently present. Thus, our main conclusion, derived from the results under isoluminance, is unlikely affected by the difference in temporal frequency for minimum-flicker adjustments. Panel (B) shows luminance factors across hue angles in each subject, which were required to equate flicker strength at 2.5 Hz. All values were normalized to that at 0 degree. These factors were measured off-line for eight colors, with the hue angle = 0, 45, 90, 135, 180, 225, 270, and 315 degrees, respectively. During the measurement, the subject adjusted the intensity of test hue to minimize the flicker strength of alternation (2.5 Hz) between the background gray with 15% luminance increase and a test hue. The average of five measurements was used. The factors for the hues in between the eight colors were linearly interpolated.

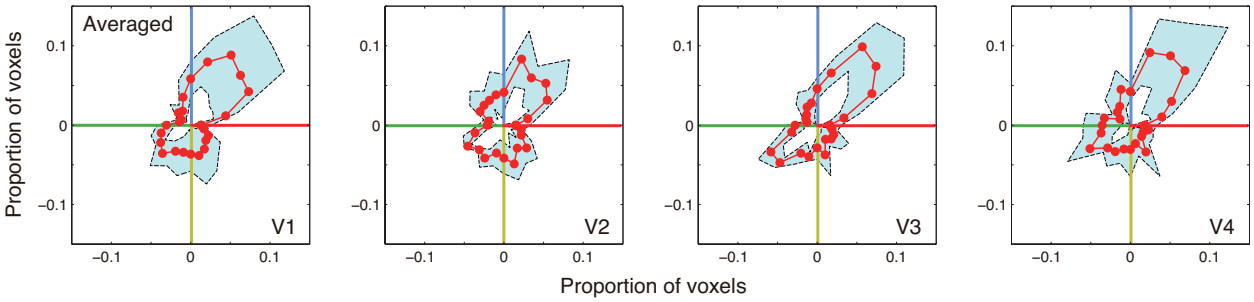

Figure S9. Comparison between hue-selective histograms with unique hues.

The mismatch between perceptual measurements (i.e., unique hues) and cone-opponent axes has been noticed in a previous psychophysics study (De Valois et al., 2000). A previous study on color representation in human visual cortex, using an fMRI decoding approach, however, has claimed that responses to unique hues can be decoded more efficiently than those to cone-opponent stimuli (Parkes et al., 2009). Similarly, single-unit recording studies in macaque monkeys have also argued for the presence of distinct neuron groups in visual cortex, each of which responds selectively to a unique hue (Stoughton and Conway, 2008; Mollon, 2009). However, the cortical origin for representing unique hues remains to be established (Mollon, 2009). We thus performed an analysis comparing hue-selective histograms with individually determined unique hues. For each subject, we determined unique hues using a psychophysical method called *method of adjustment*. Briefly, the subject adjusted the hue of a circular flickering checkerboard pattern, which was identical to the stimulus under the L_{amp} = 0.08 and S_{amp} = 0.80 condition used in the main fMRI experiment, so that the hue appeared to the subject as one of unique hues. The average hue angle for each unique hue was derived from 10 repetitions of adjustments. As shown in Figures 4A-4C, unique hues determined using this approach differed between the subjects (four dashed lines from the origin in each panel represent the *unique red*, *blue*, *green* and *yellow*, respectively). Comparing the hue angles of unique hues averaged across all subjects with averaged hue-selective angular histograms (see Figure 4D) reveals that there is no apparent correspondence between the two sets of measurements. This may be better appreciated in the figure above, where the four unique hues, measured individually and averaged across the subjects, are presented in the four major axes, and averaged angles of selective hues were normalized with respect to the unique hues. In brief, these results provide no direct evidence for the presence of neurons responding selectively to unique hues.

Supplementary Movie

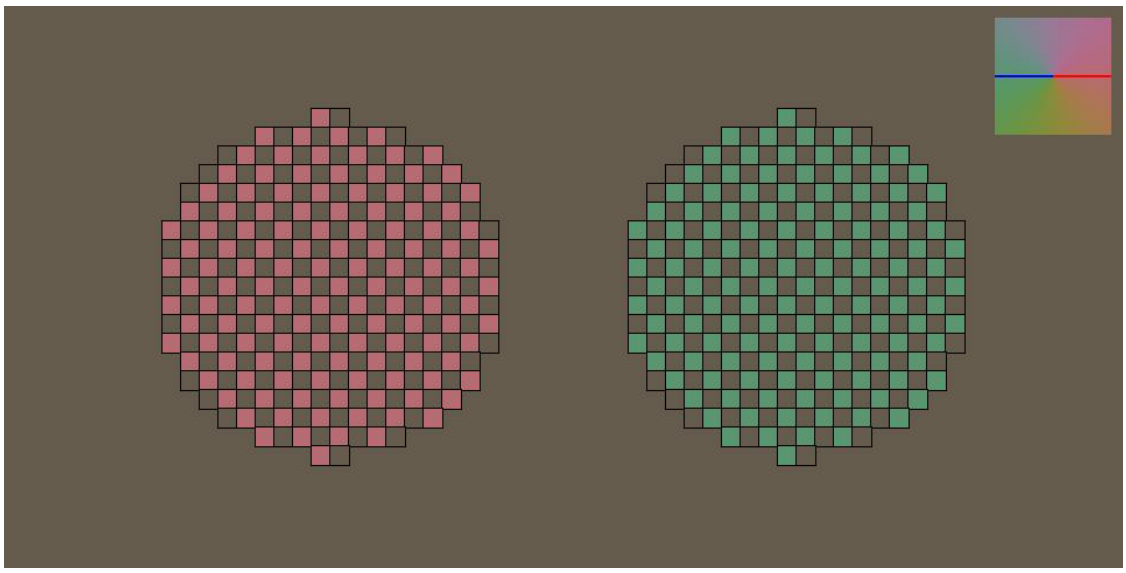

Movie S1. Continuous color changes in the stimulus.
During fMRI experiments, the stimulus colors changed continuously along the hue circle. In one block, shown on the left, the color change started from red (0° in the hue angle; see Figure 1A), and in the other block, shown on the right, the color change started from green (180°). Thus, at any given time, as illustrated by blue and red line segments in the inset, the current colors in the two blocks were always opposite to each other.

Supplementary Tables

Table S1. Numbers of selected voxels used for analyzing hue-selectivity in the present study.
Proportions of selected voxels to the total number of voxels in respective ROIs are given in parentheses

	Subject 1				Subject 2				Subject 3			
S_{amp}	V1	V2	V3	V4	V1	V2	V3	V4	V1	V2	V3	V4
0.04	72 (14.3)	41 (10.0)	52 (12.4)	22 (7.5)	97 (20.2)	80 (13.0)	70 (9.8)	48 (8.5)	174 (19.9)	26 (2.9)	46 (7.7)	22 (5.2)
0.08	169 (33.5)	72 (17.6)	7 (1.7)	51 (17.3)	114 (23.8)	79 (12.8)	61 (8.5)	48 (8.5)	137 (15.6)	14 (1.6)	40 (6.7)	12 (2.9)
0.16	107 (21.2)	33 (8.1)	51 (12.1)	27 (9.2)	58 (12.1)	36 (5.9)	39 (5.5)	26 (4.6)	156 (17.8)	23 (2.6)	52 (8.8)	14 (3.3)
0.24	163 (32.3)	45 (11.0)	55 (13.1)	49 (16.6)	137 (28.5)	117 (19.0)	107 (15.0)	80 (14.1)	135 (15.4)	21 (2.3)	28 (4.7)	18 (4.3)
0.4	146 (29.0)	52 (12.7)	51 (12.1)	44 (14.9)	103 (21.5)	69 (11.2)	71 (9.9)	71 (12.5)	176 (20.1)	29 (3.2)	45 (7.6)	21 (5.0)
0.6	197 (39.1)	71 (17.4)	100 (23.8)	67 (22.7)	111 (23.1)	75 (12.2)	69 (9.7)	56 (9.9)	116 (13.2)	20 (2.2)	37 (6.2)	9 (2.1)
0.8	157 (31.2)	60 (14.7)	63 (15.0)	49 (16.6)	75 (15.6)	47 (7.6)	54 (7.6)	32 (5.7)	311 (35.5)	68 (7.6)	127 (21.4)	41 (9.8)
average	144.4 (28.7)	53.4 (13.1)	54.1 (12.9)	44.1 (15.0)	99.3 (20.7)	71.9 (11.7)	67.3 (9.4)	51.6 (9.1)	172.1 (19.7)	38.7 (3.2)	53.6 (9.0)	19.6 (4.7)
SD	41.9 (8.3)	15 (3.7)	27.2 (6.5)	15.3 (5.2)	26.1 (5.4)	26.1 (4.2)	20.9 (2.9)	19.4 (3.4)	65 (7.4)	18 (2.0)	33.3 (5.6)	10.6 (2.5)
Number of voxels in ROI	504	408	420	295	480	615	715	566	876	895	594	420

Table S2. Statistics for the comparisons between histograms obtained from forward and reverse runs.

		between run comparisons		
Correlation coefficient test		forward	reverse	forward vs. reverse
S1	*r*	0.507	0.485	0.825
	p	0.00970	0.0139	7.05×10^{-7}
S2	*r*	0.648	*0.362*	0.413
	p	0.000466	*0.0751*	0.0447
S3	*r*	0.686	0.492	0.791
	p	0.000153	0.0124	4.19×10^{-6}
Kolmogorov-Smirnov test				
S1	χ^2	9.65	9.03	7.68
	p	0.917	0.916	0.947
S2	χ^2	7.15	7.14	14.8
	p	0.906	0.922	0.914
S3	χ^2	7.33	20.3	3.27
	p	0.912	0.886	0.962

Table S3. Average numbers and fractions of voxels that showed significant hue selectivity (corresponding to Figures 3 and 4 in the main text).
These data were obtained using the S_amp = 0.40 condition, and averaged across four runs. Proportions of selected voxels to the total numbers of voxels in respective ROIs (V1-V4) are given in parentheses.

	Subject 1				Subject 2				Subject 3			
	V1	V2	V3	V4	V1	V2	V3	V4	V1	V2	V3	V4
Number of hue selective voxels	(%)											
aveage	74.8 (14.8)	48.8 (11.9)	34.3 (8.15)	31.8 (10.8)	58.5 (11.6)	67.3 (16.5)	58.8 (14.0)	35.8 (12.1)	81.8 (16.2)	19.5 (4.78)	25.0 (5.95)	15.0 (5.08)
SD	26.3 (5.22)	16.5 (4.04)	7.09 (1.69)	11.2 (3.80)	24.7 (4.91)	15.2 (3.72)	21.8 (5.19)	13.5 (4.56)	30.8 (6.11)	7.55 (1.85)	12.7 (3.02)	4.83 (1.64)
Number of visually responsive voxels	(%)											
aveage	351.5 (69.7)	304.3 (74.6)	146.5 (34.9)	205.0 (69.5)	207.8 (43.3)	196.3 (31.9)	220.8 (30.9)	145.5 (25.7)	453.8 (46.5)	171.5 (19.2)	215.8 (35.2)	146.0 (34.0)
SD	53.54 (10.6)	68.7 (16.8)	26.6 (6.34)	26.9 (9.13)	16.7 (3.49)	65.7 (10.7)	41.1 (5.8)	50.4 (8.9)	66.6 (17.4)	32.5 (3.64)	67.9 (12.3)	17.7 (5.61)
Fraction of hue-selective voxels (%)												
average	**21.3**	**17.4**	**24.1**	**15.3**	**28.2**	**37.3**	**25.9**	**29.1**	**19.1**	**11.9**	**13.4**	**10.6**
SD	7.45	9.51	7.24	4.08	12.4	14.5	6.37	18.2	10.4	5.68	9.71	4.40
Number of voxels in ROI	504	408	420	295	480	615	715	566	876	895	594	420

References

Berens P. (2009) CircStat: a MATLAB Toolbox for Circular Statistics. J Stat Softw. 31, 1–21.

Boynton, G.M., Engel, S.A., Glover, G.H. and Heeger, D.J. (1996). Linear systems analysis of fMRI in human V1. J Neurosci, 16, 4207-4221.

De Valois, R.L., Cottaris, N.P., Elfar, S.D., Mahon, L.E., and Wilson, J.A.(2000). Some transformations of color information from lateral geniculate nucleus to striate cortex. Proc. Natl. Acad. Sci. 97, 4997-5002.

Engel, S., Zhang, X., and Wandell, B. (1997a). Colour tuning in human visual cortex measured with functional magnetic resonance imaging. Nature 388, 68-71.

Mollon, J.D. (2009) A neural basis for unique hues? Curr. Biol., 19, R441.

Mullen, K.T., Dumoulin, S.O., McMahon, K.L., de Zubicaray, G.I., and Hess, R.F. (2007). Selectivity of human retinotopic visual cortex to S-cone-opponent, L/M-cone-opponent and achromatic stimulation. Eur J Neurosci., 25, 491-502.

Parkes, L.M., Marsman, J.B., Oxley, D.C., Goulermas, J.Y., and Wuerger, S.M. (2009) Multivoxel fMRI analysis of color tuning in human primary visual cortex. J Vis 9, 1, 1–13.

Smith, V.C., and Pokorny, J. (1975). Spectral sensitivity of the foveal cone photopigments between 400 and 500 nm. Vis. Res., 15, 161-171

Stoughton, C.M., and Conway, B.R. (2008). Neural basis for unique hues. Curr Biol 18, R698-9.